New Edge Detection Enhancement Method based on Cooperation between Edge Algorithms

Ashraf A. Nijim
Faculty of Engineering
Al-Azhar University,
Cairo, Egypt.

Muhammad T. Abo Kresha Ph.D,
Faculty of Science
Al-Azhar University,
Cairo, Egypt.

Reda Abo Alez
Prof., Faculty of Engineering
Al-Azhar University,
Cairo, Egypt.

ABSTRACT
Edge detection algorithms are important tools in image processing applications for carrying out much information and being relatively easy to produce. Sobel; Canny; and logarithmic algorithms [1] are among several edge detection algorithms used frequently nowadays. The evalution of such edge detection algorithms is an old problem. Authors [1][3] tend to use visual evaluation that limits the comparison between different edge images. In this paper, we present a new edge enhancement method and five different measures that can be used to statistically evaluate edge detection algorithms. The new edge enhancement method is based on cooperation between different edge detection algorithms. The new edge preserves the advantages of each edge image. Experimental results using two edge detection algorithms proved the efficiency of this method.

General Terms
New Edge Enhancement Method; Pattern Recognition; Edge Detection Algorithms; Image Entropy; and Image Moments.

Keywords
Edge detection; Canny edge detector; Sobel edge detector; logarithmic edge detector; MSE; PSNR; PCC; Shannon Entropy; Hu-moments.

1. INTRODUCTION
Edge detection algorithms differ in their performance for different types of images. The most well- known edge detection algorithms are: Canny [1][2]; Sobel [1]; and logarithmic [1]. The performance of edge detection algorithms was evaluated in two ways: visual and numerical. Visual [1][3] means of testing the performance of edge detection algorithms has been adopted for many years because of the lack of standard measuring techniques whereas, numerical evaluation methods tend to reflect the visual difference between the object and its evaluated edge. Authors [4] and [5] used two numerical methods for evaluating the difference between two images. The Mean Square Error (MSE); the Peak Signal-to-Noise Ratio (PSNR); and Pearson's Correlation Coefficient (PCC) were used to indicate how much two images are numerically different. The entropy [8][9] and moments [10][11] of images were also used in many recognition algorithms and image processing algorithms [10][11][12].

This paper is organized as follows: Section 2 deals with edge detection algorithms. Section 3 deals with edge evaluation. Section 4 presents the new edge enhancement method. Section 5 deals with the edge evaluation results. Section 6 deals with the new edge enhancement results. Section 7 deals with the discussion part of the results, and Section 8 deals with the conclusions of this study.

2. EDGE DETECTION ALGOITHMS
Authors [13][14] provided different definitions for the edge of a given image. The definition of an edge for a given object that best satisfies our study purpose is: An edge is a set of connected pixels of width one that lies on the boundary of two regions. Inner-edge is the boundary of some region that lies inside the edge of that region. And, the outer-edge is the set of pixels that lies exactly outside the boundary of a region.

In the following section, three different edge detection algorithms will be described.

2.1 Sobel Edge Detector
The Sobel edge detector [1] is a simple non-linear edge detection technique. It uses two 3X3 filters to find the differencing scheme in an image.

$Let\ a \in \mathbb{R}^X\ be\ the\ source\ image, and$

$Let\ m \in \mathbb{R}^X\ be\ the\ gradient\ magnitude\ image$

Then, Sobel edge magnitude image m is defined as follows:-

$$m(i,j) := \sqrt{(a \oplus s)^2 + (a \oplus t)^2},$$

where the templates s and t are defined as follows:-

$$s = \begin{matrix} -1 & -2 & -1 \\ 0 & 0 & 0 \\ 1 & 2 & 1 \end{matrix}, and\ \ t = \begin{matrix} -1 & 0 & 1 \\ -2 & 0 & 2 \\ -1 & 0 & 1 \end{matrix}$$

The gradient direction d could be found using the following formula:-

$$d = arctan2((a \oplus s)|_{m>0}, (a \oplus t)|_{m>0})$$

2.2 Canny Edge Detector
Canny edge detection [1][2] is a multi-stage image processing algorithm. The squared gradient magnitude is computed first. Edges are then identified as the local maxima of this magnitude if its value exceeds a predefined threshold. Canny's algorithm was designed to achieve three optimization constrains:-

i. Good detection by maximizing the signal to noise ratio.
ii. Good localization to accurately mark edges.
iii. Respond only once to a single edge in a 1-D signal.

2.3 Logarithmic (Wallis) Edge Detector
The logarithmic edge detection [1] uses the difference between the log value of a given pixel and its neighbors to find the edge pixels. If the value exceeds a predefined threshold then this pixel is an edge pixel.

$Let\ a \in \mathbb{R}^X\ be\ the\ sourse\ image, and$

$a_0, a_1, a_2, a_3\ are\ the\ 4 - neighbors\ of\ the\ pixel\ in\ (i,j),$

the edge image $b \in \mathbb{R}^X$ is given by,

$$b(i,j) = \log_b\big(a(i,j)\big) - \frac{1}{4}(\log_b(a_0) + \log_b(a_1) + \log_b(a_2) + \log_b(a_3))$$

The previous equation can be extended to include more than 4-neighbors for wider comparison.

3. EDGE EVALUATION

Following are five image techniques used to statistically evaluate images:

3.1 MSE

The Mean Square Error (MSE) [4] for two images I and K is defined as follow:-

$$MSE = \frac{1}{m*n}\sum_{i=0}^{m-1}\sum_{j=0}^{n-1}[I(i,j) - K(i,j)]^2 ,$$

Where $m * n$ is the size of the image.

3.2 PSNR

The Peak Signal-to-Noise Ratio ($PSNR$) [5] is defined as follows:-

$$PSNR = 10\ \log_{10}(\frac{MAX^2}{MSE}),$$

where MAX is the maximum pixel value the image can have.

3.3 Pearson's Correlation Coefficient (PCC)

The Pearson's Correlation Coefficient (PCC)[17][18] is defined as follows:-

$$PCC = \frac{\sum_i (x_i - x_m)(y_i - y_m)}{\sqrt{\sum_i (x_i - x_m)^2}\sqrt{\sum_i (y_i - y_m)^2}},$$

Where,

x_i is the intensity of the i^{th} pixel in image1,

y_i is the intensity of the i^{th} pixel in image2,

x_m is the mean intensity of image1, and

y_m is the mean intensity of image2.

The correlation coefficient returns a value between 1 and -1. A value of 1 indicates that the two images are identical, a 0 that the images are completely uncorrelated, and -1 indicates that the images are completely anti-correlated for example if the image is a negative of the other.

3.4 Central Moments

The central moments μ_{pq} [11] of a function $f(x,y)$ are defined as follows:-

$$\mu_{pq} = \int_{a_1}^{a_2}\int_{b_1}^{b_2}(x-\bar{x})^p(y-\bar{y})^q\ f(x,y)dx\ dy,$$

where $\bar{x}$ and $\bar{y}$ are the coordinates of the center of mass.

This entropy is invariant for image translation coordinates. Hu [10] [11] describes a combination of seven moments $\phi_1 - \phi_7$ derived from central moments. Those moments proved to be invariant to scaling; orientation; and position changing. The first four Hu moments are as follows:-

$$\phi_1 = \mu_{20} + \mu_{02}$$

$$\phi_2 = (\mu_{20} - \mu_{02})^2 + 4\mu_{11}^2$$

$$\phi_3 = (\mu_{30} - 3\mu_{12})^2 + (3\mu_{21} - \mu_{03})^2$$

$$\phi_4 = (\mu_{30} - \mu_{12})^2 + (\mu_{21} - \mu_{03})^2$$

3.5 Shannon Entropy

Shannon entropy [8][9]is defined as a measure of the average information content associated with a random outcome.

Shannon entropy $H(X)$ for discrete random variable X, with possible states $x_1, x_2, \dots, x_n$ is defined as follows:-

$$H(X) = \sum_{i=1}^{n} p(x_i)\log_2\left(\frac{1}{p(x_i)}\right) = -\sum_{i=1}^{n} p(x_i)\log_2 p(x_i),$$

where, $p(x_i) = Pr(X = x_i)$ is the probability of the i^{th} outcome of X.

4. NEW ENHANCEMENT METHOD

The proposed new edge enhancement method is based on different edge detection algorithms selection. Two or more of well-known edge detection algorithms coordinate to find a new edge. The new edge reserves the benefits of each of those edge algorithms. The edge enhancement method is composed of three steps: The first step is referred as the x-direction edge selection. The pseudo code for this step is as follows:-

For each place (pixel) in the new edge image:

- Check if the pixels in the right side x-direction of the different n-edge images have one or more edge pixel, if True, then;
- Check if the pixels in the left side x-direction of the different n-edge images have one or more edge pixel, if True, then;
- Set that pixel to black-edge pixel (see Figure 2).

Fig 1: The pseudo code for the x-direction edge selection

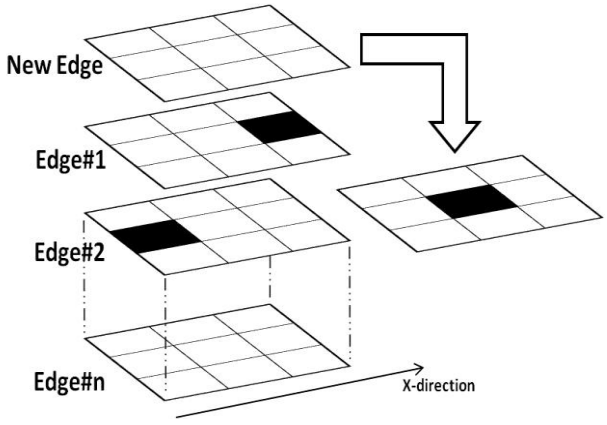

Fig 2: First step, x-direction edge selection

The second step is referred as the y-direction edge selection. The pseudo code for this step is as follows:-

For each white (non-edge) place in the new edge image:

- Check if the pixels in the right side y-direction of the different n-edge images have one or more edge pixel, if True then;
- Check if the pixels in the left side y-direction of the n-edge images have one or more edge pixel, if True, then;
- Set that white pixel to black-edge pixel (see Figure 4).

Fig 3: The pseudo code for the y-direction edge selection

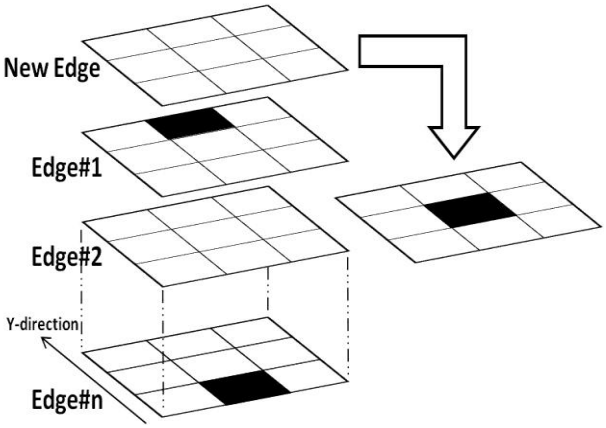

Fig 4: Second step, y-direction edge selection

The third and final step is a post edge enhancement step. In this step the new edge image is investigated to remove any artifacts during the two selection steps and to make sure that the new edge is of one pixel width.

5. EDGE EVALUATION RESULTS

In this section, we will investigate the relationship between the original image and its edge images. Three edge detection algorithms –Sobel; Canny; and logarithmic- are used on two groups of image. The first group is composed of binary images with different geometric shapes (see Figure 5). The second group of images is a database of colored retina images [6][7]. A sample of this database is shown in Figure 6. Evaluation was done using the five methods presented in section 3. A Sample of the results from the first group of images is presented in Table 1. (Geom1) binary image was evaluated with its three edge images.

Fig 5: Geometric shapes test image (Geom1)

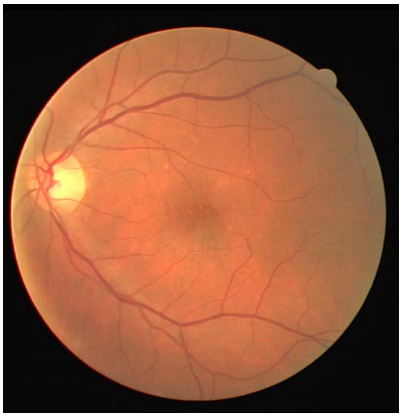

Fig 6: Retina test image, 21_training.tif (Ret2)

The comparison results for both images are shown in Table 1 and Table 2.

Table 1. Test image (Figure 5) evaluation results

Test\Image	Original	Canny	Sobel	Log.
MSE	---	9384	9425	9637
PSNR	---	69.990	69.971	69.874
PCC	---	0.0800	0.0630	-0.0142
Shannon Entropy	0.6849	0.1507	0.1505	0.1589
Hu Moments (ϕ_1)	0.2183	0.1675	0.1675	0.1675
Hu Moments (ϕ_2)	3.5778	3.6720	3.6720	3.6719
Hu Moments (ϕ_3)	1.6784	3.9394 x10^{-4}	3.7803 x10^{-4}	4.4733 x10^{-4}
Hu Moments (ϕ_4)	12.0395	7.1347 x10^{-4}	7.1164 x10^{-4}	13.2040 x10^{-4}

Sample evalution results for the second group of images are presented in Table 2. Ret2 gray scaled image was evaluated with its three edge images.

Table 2. Retina image (Figure 6) evaluation results

Test\Image	Original	Canny	Sobel	Log.
MSE	---	18950	17594	18390
PSNR	---	60.539	60.861	60.669
PCC	---	-.1490	.0190	-.1103
Shannon Entropy	6.4890	1.7072	.3214	1.4177
Hu Moments (ϕ_1)	0.1950	0.1801	0.1675	0.1740
Hu Moments (ϕ_2)	3.6224	3.6374	3.6613	3.6486
Hu Moments (ϕ_3)	0.5944	1.4127 x10^{-2}	1.7038 x10^{-4}	1.2215 x10^{-2}
Hu Moments (ϕ_4)	1.1236	10.660 1 x10^{-2}	3.9537 x10^{-4}	1.1873 x10^{-2}

Evaluation results of both previously mentioned images after transformation techniques are shown in Table 3 for the first test image (Geom1), and Table 4 for the retina image (Ret2). Both images were scaled-up twice (see Table 3 d), and (see Table 4 d); and scaled-down to half of its original size (see Table 3 e), and (see Table 4 e). Three rotation results are also presented: 20 degrees clock wise (see Table 3 a) and (see Table 4 a); 45

degrees CW (see Table 3 b) and (see Table 4 b); and 70 degrees CW (see Table 3 c) and (see Table 4 c).

Table 3. Test image (Figure 1) comparison results

(a) Rotation 20° CW

Test\Image	Original	Canny	Sobel	Log.
MSE	---	9422	9407	9594
PSNR	---	69.972	69.979	69.894
PCC	---	0.0699	0.0609	0.0021
Shannon Entropy	0.8310	0.2227	0.1736	0.1948
Hu Moments (ϕ_1)	0.2183	0.1679	0.1675	0.1677
Hu Moments (ϕ_2)	3.5800	3.6712	3.6720	3.6717
Hu Moments (ϕ_3)	1.6777	9.1944 x10^{-4}	3.5178 x10^{-4}	4.9706 x10^{-4}
Hu Moments (ϕ_4)	17.5424	21.396 2 x10^{-4}	8.1267 x10^{-4}	14.523 3 x10^{-4}

(b) Rotation 45° CW

Test\Image	Original	Canny	Sobel	Log.
MSE	---	9411	9413	9582
PSNR	---	69.977	69.976	69.899
PCC	---	0.0740	0.0585	0.0050
Shannon Entropy	0.8377	0.2373	0.1849	0.2081
Hu Moments (ϕ_1)	0.2183	0.1679	0.1674	0.1676
Hu Moments (ϕ_2)	3.5795	3.6712	3.6721	3.6717
Hu Moments (ϕ_3)	1.6757	10.160 7 x10^{-4}	3.6387 x10^{-4}	6.5088 x10^{-4}
Hu Moments (ϕ_4)	19.0190	16.178 8 x10^{-4}	8.6183 x10^{-4}	11.536 5 x10^{-4}

(c) Rotation 70° CW

Test\Image	Original	Canny	Sobel	Log.
MSE	---	9418	9410	9589
PSNR	---	69.974	69.978	69.896
PCC	---	0.0696	0.0582	1.2165 x10^{-4}
Shannon Entropy	0.8330	0.2273	0.1796	0.1944
Hu Moments (ϕ_1)	0.2183	0.1679	0.1674	0.1676
Hu Moments (ϕ_2)	3.5760	3.6711	3.6720	3.6716
Hu Moments (ϕ_3)	1.6794	8.3108 x10^{-4}	4.0501 x10^{-4}	5.9954 x10^{-4}
Hu Moments (ϕ_4)	17.0861	18.289 4 x10^{-4}	8.3968 x10^{-4}	14.101 8 x10^{-4}

(d) Scaling 2X

Test\Image	Original	Canny	Sobel	Log.
MSE	---	9437	9432	9528
PSNR	---	75.986	75.988	75.944
PCC	---	0.0418	0.0444	0.0114
Shannon Entropy	0.6849	0.0846	0.0854	0.1320
Hu Moments (ϕ_1)	0.2183	0.1670	0.1670	0.1673
Hu Moments (ϕ_2)	3.5778	3.6728	3.6728	3.6724
Hu Moments (ϕ_3)	6.7137	4.0329 x10^{-4}	4.0919 x10^{-4}	7.2858 x10^{-4}
Hu Moments (ϕ_4)	48.1580	7.5674 x10^{-4}	7.6264 x10^{-4}	47.395 5 x10^{-4}

(e) Scaling 0.5X

Test\Image	Original	Canny	Sobel	Log.
MSE	---	9440	9450	9664
PSNR	---	63.944	63.939	63.842
PCC	---	0.0663	0.0641	0.0069
Shannon Entropy	0.7735	0.2751	0.2799	0.2909
Hu Moments (ϕ_1)	0.2183	0.1683	0.1683	0.1683
Hu Moments (ϕ_2)	3.5778	3.6705	3.6705	3.6705
Hu Moments (ϕ_3)	0.4196	3.7567 x10^{-4}	3.9048 x10^{-4}	4.0574 x10^{-4}
Hu Moments (ϕ_4)	3.0094	7.0772 x10^{-4}	7.6352 x10^{-4}	8.2237 x10^{-4}

Table 4. Retina image (Figure 2) comparison results

(a) Rotation 20° CW

Test\Image	Original	Canny	Sobel	Log.
MSE	---	20793	19487	20329
PSNR	---	60.136	60.417	60.234
PCC	---	-.1450	-.0011	-.1177
Shannon Entropy	6.5123	1.7612	0.3770	1.4350
Hu Moments (ϕ_1)	0.1934	0.1803	0.1677	0.1747
Hu Moments (ϕ_2)	3.6153	3.6361	3.6607	3.6475
Hu Moments (ϕ_3)	0.5413	2.0446 x10^{-2}	4.4937 x10^{-4}	2.6411 x10^{-2}
Hu Moments (ϕ_4)	1.2305	15.850 5 x10^{-2}	43.934 9 x10^{-4}	8.9174 x10^{-2}

(b) Rotation 45° CW

Test\Image	Original	Canny	Sobel	Log.
MSE	---	21640	20226	21088
PSNR	---	59.962	60.256	60.074
PCC	---	-.1599	5.2006	-.1212

			x10^{-4}	
Shannon Entropy	6.4254	1.7697	0.3680	1.4245
Hu Moments (ϕ_1)	0.1929	0.1805	0.1677	0.1747
Hu Moments (ϕ_2)	3.6086	3.6357	3.6610	3.6479
Hu Moments (ϕ_3)	0.5872	1.0556 x10^{-2}	2.9235	2.2604 x10^{-2}
Hu Moments (ϕ_4)	2.2153	0.2552	42.047 5 x10^{-4}	0.1320

(c) Rotation 70° CW

Test\Image	Original	Canny	Sobel	Log.
MSE	---	20785	19497	20383
PSNR	---	60.137	60.415	60.222
PCC	---	-.1407	3.8123 x10^{-4}	-.1231
Shannon Entropy	6.5236	1.7892	0.3728	1.4675
Hu Moments (ϕ_1)	0.1934	0.1804	0.1677	0.1749
Hu Moments (ϕ_2)	3.6102	3.6359	3.6610	3.6470
Hu Moments (ϕ_3)	0.6429	68.254 5 x10^{-4}	3.1777	1.4964 x10^{-2}
Hu Moments (ϕ_4)	3.0342	0.3283	33.279 1 x10^{-4}	0.1652

(d) Scaling 2X

Test\Image	Original	Canny	Sobel	Log.
MSE	---	18730	17594	18438
PSNR	---	66.616	66.882	66.678
PCC	---	-.1417	-.0052	-.1187
Shannon Entropy	6.4805	1.5674	0.2318	1.6274
Hu Moments (ϕ_1)	0.1950	0.1779	0.1673	0.1794
Hu Moments (ϕ_2)	3.6224	3.6411	3.6616	3.6378
Hu Moments (ϕ_3)	2.3777	4.0783 x10^{-2}	10.751 1 x10^{-4}	2.9505 x10^{-2}
Hu Moments (ϕ_4)	4.4936	0.2179	30.357 5 x10^{-4}	0.1826

(e) Scaling 0.5X

Test\Image	Original	Canny	Sobel	Log.
MSE	---	19250	17586	18207
PSNR	---	54.442	54.835	54.684
PCC	---	-0.1663	0.0443	-0.0817
Shannon Entropy	6.4927	1.8969	0.4716	1.1199
Hu Moments (ϕ_1)	0.1950	0.1826	0.1678	0.1715
Hu Moments (ϕ_2)	3.6217	3.6307	3.6599	3.6529
Hu Moments (ϕ_3)	0.1495	1.0039 x10^{-2}	1.6742 x10^{-5}	0.2850 x10^{-2}
Hu Moments (ϕ_4)	0.2798	3.3730 x10^{-2}	5.2696 x10^{-5}	0.5355 x10^{-2}

6. NEW EDGE ENHANCMENT RESULTS

The new method was tested using three images. The true edges of those images were extracted manually. The first test image is the binary image (Geom1) which has five different geometric shapes. The size of this image is 1200x1200 pixels (see Figure 5).

The two other test images are texture mosaic images from the USC-SIPI web site database[15][16] (see Figure 7 and Figure 8).

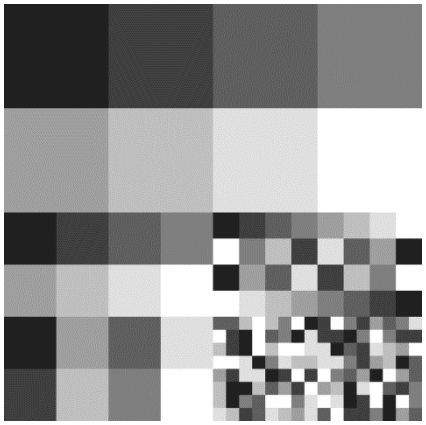

Fig 7: Texture Mosaic Image, texmos2.s512.tiff (Texm1)

Fig 8: Texture Mosaic Image, texmos3.s512.tiff (Texm2)

Two edge detection algorithms, Canny and Sobel have been used to produce the new proposed edge image. Comparison results between the three edge images and the manually-produced true-edge images are shown in Table 5.

Table 5. Canny, Sobel and the new edge comparison results

Image name	Test/ Edge Alg.	Canny vs. True Edge	Sobel vs. True Edge	NewEdge vs. True Edge
Geom1	MSE	2288×10^{-6}	2930×10^{-6}	2261×10^{-6}
	PSNR	87.9886	86.9141	88.0390
Texm1	MSE	4082×10^{-5}	3711×10^{-5}	4077×10^{-5}
	PSNR	68.0757	68.4901	68.0818
Texm2	MSE	1512×10^{-5}	1611×10^{-5}	1508×10^{-5}
	PSNR	72.3894	72.1135	72.3993

The comparison results showed an improvement in the new edge image compared to both Canny and Sobel edge images. The MSE was reduced, showing that the two edge images – the new edge image and the true edge image – are getting closer to each other. The Sobel edge results for the texture mosaic image (Texm1) is found to be better than both Canny and the New Edge images. This result is expected because Sobel edge detection algorithm proved to give accurate detection for edges parallel to the x and y directions. In this special case, (Texm1) has all of its edges parallel to either the x or the y directions (see Figure 6).

Figure 9 shows parts from the first test image (Geom1). The resulting new edge image has improved. Corners and oblique lines are closer to the original image than both edge detection algorithms - Canny and Sobel. Even more, the new method improved the Sobel edge by adding the missing pixels from the edge.

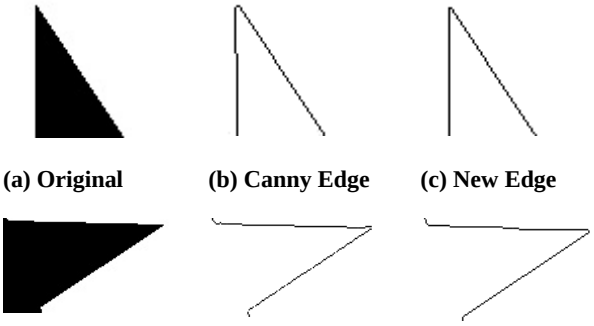

(a) Original **(b) Canny Edge** **(c) New Edge**

(a) Original **(b) Sobel Edge** **(c) New Edge**

Fig 9: Edge enhancement, (a) Parts from (Geom1) (Figure 5); (b) Edge detection results using Canny and Sobel; (c) New edge enhancement image.

7. DISCUSION

The MSE values between the original image and its edge images represent the inner non-edge pixels of the objects in the image, and the edge identification errors. Those errors include misplaced edges and noise added by the edge identification algorithm. The value of MSE is greater than zero sincea zero MSE value is only found when comparing two identical images. MSE between the edge and its original image does not change with rotation or scaling for simple geometric shapes (see Figure 5). This value slightly changes with complex images (see Figure 6). From our observation this change did not exceed 4%.

The PSNR represents a ratio of change for two images to the maximum possible value of an image. The same discussion can be said about the PSNR. However, the change of PSNR values after rotation and scaling didn't exceed 1% for both simple and complex images. This makes the PSNR value more favorable.

The value of the PCC proved that the edge images and the original image are not correlated. The PCC values are close to zero for both images. Most of the values are positive for the first image (Geom1) but negative for the second image (Ret2).

The edge image doesn't provide that much information as the original image provides. This explains the great change in entropy value between the original image and the different edge images.

The first and the second Hu-moments (ϕ_1 *and* ϕ_2) of the images is observed to have the same value for the different edge images (see Table 1, and Table3) for simple geometric shapes. For complex images those values start to set apart. But, the second Hu-moments (ϕ_2) was observed to have identical values with the original image moments after scaling (see Table 4 d and e). The second Hu-moments for the complex retina image (Ret2) and its three edge images were observed to have common values.

The new edge enhancement results showed that the new proposed method improved edge detection. The cooperation between two or more edge detection algorithms using relatively simple techniques provided better edge detection. Using only two edge images, better angles and oblique lines detection were achieved. The MSE and PSNR values proved this improvement for the two sample images. Both values have been computed using manually generated true edge images. Those true edge images may not represent the true edge for some algorithms because of inconsistency in defining edges.

8. CONCLUSION

Cooperation between two or more edge detection techniques proved to give better edge detection. The results after using the new method with two edge detection algorithms showed a significant improvement in edge detection. The angles and oblique lines of Canny and Sobel edge images were properly detected. Statistical results using manually generated true edge images showed that the new edge image and the true image were closer than both edge images.

MSE and PSNR between edge images and the original image were observed to have identical values under rotation and scaling. Difference in those values represents the change in edge detection for two algorithms. The higher the MSE value, the more complex the image is. Shannon entropy [8][9] value for the edge images is lower than the entropy of the original image. This is due to the fact that the edge image does not carry that much information the original image does.

Hu [10][11] first and second moments observed to have common values for the three edge images but with slight change represent the difference in edge detection. This observation was noticed for simple shape images. For complex images the values of the second Hu-moments for the edge images and the original image observed to be have comment values under scaling.

9. REFERENCES

[1] Ritter, G. X., and Wilson J. N. 2001. Handbook of Computer Vision Algorithms in Image Algebra. Second Edition. CRC Press.

[2] Ali, M., and Clausi, D. 2001. Using The Canny Edge Detector for Feature Extraction and Enhancement of Remote Sensing Images. IEEE Geoscience and Remote Sensing Symposium. 2298-2300.

[3] Shrivakshan, G.T., and Chandrasekar, C., 2012. A Comparison of various Edge Detection Techniques used in Image Processing. IJCSI International Journal of Computer Science Issues, Vol. 9, Issue 5, No 1. 269-276.

[4] Tan, H. L., Li, Z., Tan, Y. H., Rahardja, S., and Yeo C. 2013. A perceptually Relevant MSE-Based Image Quality Metric. IEEE Transactions on Image Processing, Vol. 22, No. 11. 4447-4459.

[5] Huynh-Thu, Q., and Ghanbari, M. 2008. Scope of validity of PSNR in image/video quality assessment. Electronic Letters, Vol. 44, Issue 13. 800-801.

[6] Staal, J.J., Abramoff, M.D., Niemeijer, M., Viergever, M.A., and van Ginneken, B. 2004. Ridge based vessel segmentation in color images of the retina. IEEE Transactions on Medical Imaging, vol. 23. 501-509.

[7] Niemeijer, M., Staal, J.J., van Ginneken, B., Loog, M., and Abramoff, M.D. 2004. Comparative study of retinal vessel segmentation methods on a new publicly available database. SPIE Medical Imaging, Vol. 5370. 648-656.

[8] Shannon, C. E. 1948. A Mathematical Theory of Communication. Bell System Technical Journal, 27 (3). 379–423.

[9] Shannon, C. E., and Weaver, W. 1949. The Mathematical Theory of Communication. University of Illinois Press.

[10] Hu, M. K. 1961. Pattern recognition by moment invariants, Proc. IRE49. 1428.

[11] Hu, M. K. 1962. Visual problem recognition by moment invariant. IRE Trans. Inform. Theory. Vol. IT-8. 179-187.

[12] Rizon, M., Yazid, H., Saad, P., Shakaff, A. Y., Saad, A., Mamat, M. R., Yaacob, S., Desa, H., and Karthigayan, M. 2006. Object Detection using Geometric Invariant Moment. American Journal of Applied Science 2 (6). 1876-1878.

[13] El-Sayed, M. 2011. A New Algorithm Based Entropy Threshold for Edge Detection in Images. IJCSI International Journal of Computer Science Issues. Vol. 8, Issue 5, No 1. 71-78.

[14] Vidya, P., Veni, S., and Narayanankutty K. A. 2009. Performance Analysis of Edge Detection Methods on Hexagonal Sampling Grid. International Journal of Electronic Engineering Research. Vol. 1, No. 4. 313-328.

[15] Signal and Image Processing Institute. The USC Texture Mosaic Images. USC University of Southern California. http:// sipi.usc.edu.

[16] Laws, K. I. 1980. Textured Image Segmentation. PhD thesis, University of Southern California. USCIPI. Report 940.

[17] Neto, A. M., Rittner, L., Leite, N., Zampieri, D. E., Lotufo, R., and Mendeleck, A. 2007. Pearson's Correlation Coefficient for Discarding Redundant Information in Real Time Autonomous Navigation System. IEEE Multi-conference on Systems and Control, Cingapura.

[18] Neto, A. M., Victorino, A. C., Fantoni, I., and Zampieri, D.E. 2011, Automatic Regions-of-Interest Selection based on Pearson's Correlation Coefficient. IROS Workshop on Visual Control of Mobile Robots (ViCoMoR), San Francisco, USA.